



A SURVEY ON STRENGTHENING OF REINFORCED CONCRETE BEAMS UNDER STATIC AND IMPACT LOADS

Received: 28-04-2025

Accepted: 01-06-2025

Amira Elnagar ^a, Sabry Fayed ^b, Ali Basha ^b

^a Civil Engineering Department, Higher Institute of Engineering, King Mariot, Alexandria, Egypt

^b Civil Engineering Department, Faculty of Engineering, Kafrelsheikh University, Kafrelsheikh, Egypt

* Corresponding author: A. Elnagar (Amira.elnagar.2016@gmail.com)

ABSTRACT. In general, strengthening and rehabilitation are needed for the structural components of reinforced concrete (RC) buildings and bridges, particularly the beams. Environmental factors, adjustments to the original use that caused higher applied loads, or structural upgrades to adhere to and implement the latest design rules and principles. Throughout their service lives, reinforced concrete beams most likely encounter several types of impact loading. Because such impact loading may destroy the entire structure, human life is in danger. In this survey, drop weight loading is used to increase the impact performance of reinforced concrete structures. RC strengthened beams were tested and impacted with different techniques of drop weight and different heights. The key variables in the study were the drop height, drop hammer, and cross-sectional measurements. It was found that RC beams behaved differently when subjected to static loading in contrast subjected to impact loads. For reinforced concrete buildings, increasing the drop height greatly enhanced the sustained blows. Providing a strengthening layer in the tension side and using sustainable internal reinforcement reveal the best structural behavior over the structure's service life.

KEYWORDS: Drop hammer; low-velocity impact; repair, Strengthening, Beams.

1. INTRODUCTION

Terrorism Numerous experts have noted the beam elements' dynamic reactivity as a result of the design specifications meant to protect structures from impact loads. It is difficult to design reinforced concrete beams to be protective against impact loading. The most susceptible to collisions with cars include, for instance, the columns of bridges, the columns of buildings with fewer than three stories, and roadside features like traffic signal structures and parapets [1]. When subjected to impact loads, structural elements' response and mode of failure differ significantly from those of static loads. When structural elements are damaged, reorienting the bridges and strengthening the structures is required to prevent further damage and save a significant economic cost. Another possible outcome would be the loss of priceless human life. Thus, it is crucial to properly design, safeguard, and reinforce these structures against impact loads. Drop-weight impact tests come in a wide variety of parameters and varieties that can greatly affect how RC beams respond to impacts. For instance, when Drop-weight head geometry was used, distinct reactions were

obtained even if the drop weight and impact velocity were the same [2].

Previous investigations used RC beams that were simply supported at the boundary, and drop weight was placed onto the RC beams at mid-span at a predefined height according to the planned impact velocity. The load cell was either placed on the impacted beams or included within the drop weight [3, 4] to calculate the impact force between the RC beams and the drop weight [5] as shown in Fig. 1. Various drop weight head designs, including hemispherical [3, 7, 8], flat [4, 6, 7, 9, 10], wedge [11], and curved surfaces with varying radius of curvature [12, 13], were utilized in the testing as outlined in the introduction in Table (1) and Table (5). Furthermore, the situation of impacting the drop weight directly [15, 41], or onto different impact intermediaries between RC beams and drop weights, such as steel plates [3], rubber pads [11], steel plates coupled with rubber pads [9, 10], or plywood mats [7], as observed in Table (1).

Recent studies on rapid expansion have focused on ultra-high performance concrete (UHPC). Like normal-strength concrete (NSC), ultra-high-

performance concrete (UHPC) has an extraordinarily low water-to-binder ratio and an intense microstructure. UHPC has significant tensile strength by increasing the steel fiber content that will be a good behavior under impact loading. UHPC beams under low-velocity drop weight loading had been investigated by [17,18]. It was determined how many different factors, including impact energy, span length, fiber content, and reinforcement ratio, affected the shear resisting capability. According to test results, UHPC beams showed better resistance to impacts. Experimental observations were made of a sizable RC beam reinforced with a UHPC layer on the compressive side and exposed to four-point bending tests [19,20]. Research confirmed that the UHPC layer optimized the flexural mechanism, successfully controlled the fracture distribution, and improved service condition stiffness. The influence of strengthening sites (upper or lower) and layer depth on combination RC-UHPC beams was seen during

four-point flexural testing [21]. Bottom reinforced beams outperformed top reinforced beams in terms of flexural efficiency, and the optimum load capability grew with the depth of the compression UHPC layer, whereas flexibility increased with

the depth of the tension layer. Experimental research has examined the flexural behavior of RC-UHPC composite beams that were strengthened with three schemes: tensile side strengthening, two longitudinal side strengthening, and three sides [22]. Sandblasting and smoothing with epoxy glue were the techniques used as interface preparation. The surface strengthening beams with sandblasting were found to exhibit superior flexural performance. Furthermore, the specimens with tensile side strengthening exhibited the least rise in flexural capacity. However, the RC beams with UHPC layer enhancing on each side exhibited the largest enhancement.

Table 1. Outlined the drop weight head geometries and impact interlayer from earlier studies

Reference	Drop weight head geometry	Impact interlayer	Figure of test setup
Kishi et al. [13]	Curved surface, R = 1407 mm	Direct impact	Fig. 1a
Saatci & Vecchio [6]	Flat surface	Steel plate, 50 mm thick, 305 mm wide	Fig. 1b
Chen & May [7]	a. Hemispherical surface width of (R = 125 mm). b. Flat surface	a. Direct. b. Plywood of 12 mm thick	Fig. 1c
Fujikake et al. [15]	Hemispherical	Direct impact	Fig. 1d
Tachibana et al. [12]	Curved surface	Direct impact	Fig. 1e
Yilmaz et al. [10]	Flat surface	Steel plate supported with hard rubber pad	Fig. 1f
Zhan et al. [11]	Wedge with 30 x 80 mm rectangle flat surface	Rubber pad of 3 mm in thickness	Fig. 1g
Adhikary et al. [8]	Hemispherical surface with radius of 90 mm	Direct impact	Fig. 1h
Anil et al. [9]	Flat surface	Steel plate of 10 mm in thickness and 40 mm in width along with rubber pad	Fig. 1i
Zhao et al. [3]	Hemispherical surface with radius of 500 mm	Square steel plate of 30 mm in thickness and 200 mm in width	Fig. 1j
Yan et al. [4]	Flat surface	Direct impact	Fig. 1k



Fig. 1a



Fig. 1b

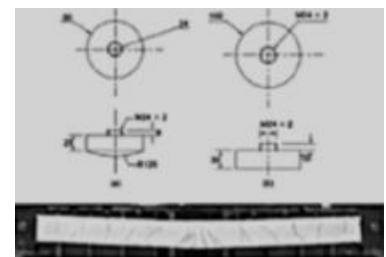


Fig. 1c

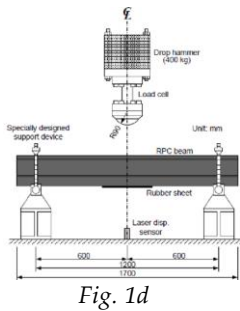


Fig. 1d

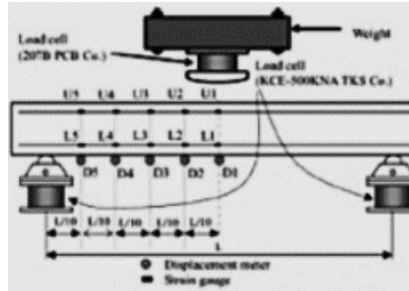


Fig. 1e



Fig. 1f



Fig. 1g



Fig. 1h

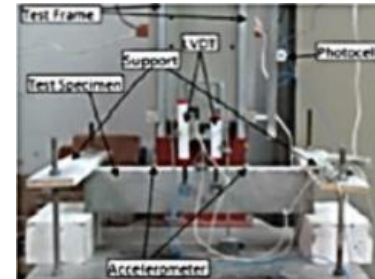


Fig. 1i

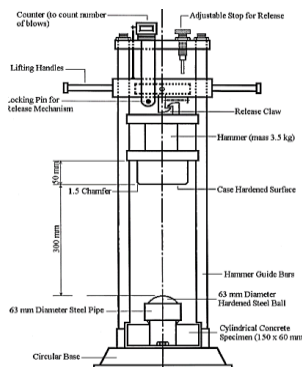


Fig. 1j



Fig. 1k

Fig. 1 Test setup

Several studies investigated drop weight tests to classify the collision mechanism from static flexural failure type RC beams [24,25,26,28,29]. Thirty RC beams had been tested for static flexural and falling weight impact tests for deciding the residual conduct of the beams [27]. A finite-element investigation with a parametric optimization had been observed. The results showed that impact damage affected the flexural strength and secant stiffness of most RC beams, but strain hardening improved flexural strength. Furthermore, the effect of the transverse reinforcement ratio improved from 0.11% to 0.56%. The results indicated that the higher stirrup quantity rewarded higher residual resistance due to the confinement effect. An experimental investigation aimed at enhancing comprehension of impact-damaged buildings' residual performance has been made public [23]. The study investigated how impact damage affects the residual behavior of reinforced concrete (RC) beams through static load testing. Twenty-nine RC beams were experimentally investigated; eight beams were kept intact, while the other twenty-one were exposed to collision loading using falling weight. This causes damage prior to future static flexural assessment. The effect of collision

fracture on the residual behavior of reinforced concrete (RC) beams through static loading had been investigated by the current study. Although their flexural characteristics were not substantially distinct, it was discovered that the collision fractured RC beams' bending rigidity and displacement ductility were significantly reduced.

2. EXPERIMENTAL PROGRAM ON IMPACT-DAMAGE INFLUENCE ON RC BEAMS

2.1. DESCRIPTION OF TEST SPECIMENS

The dimensions of the RC beam specimens studied [16] are as follows: 250 mm depth, 150 mm width, and 1,700 mm length. The experimental study has examined parameters such as drop height in drop hammer impact tests, and analyzed how varying the length of longitudinal steel reinforcement influences the response of RC beams. Among the 21 RC beams, 15 beams (Specimen groups 1- 4) were analyzed to examine impact behavior and produce a predictive formula for the maximum deflection of RC beams subjected to drop weight impact tests [30]. The

remaining 9 beams (Specimen groups 6 - 8) were studied by [31] to enhance the prediction formula suggested in [30] and investigate the impact behavior's relationship to flexural stiffness.

The five variables covered in the dropping weight test were impact energy, cross-section size, flexural ability, drop weight progress, and the RC beam's concrete compressive strength. Among the earlier studies [32 - 34], two of the five mentioned qualities, collision energy and flexural ability, have a significant effect on collision response. Two collision energy levels, 30 kJ and 50 kJ, selected based on previous investigations and the energy levels associated with rockfall on roadways. Two fixed flexural strengths of the RC beams, 700 and 937 kN, were chosen in light of the higher impact energy level in comparison to earlier research. The study investigates how the motion of the dropping weight and the resulting velocity influence the collision reaction of RC beams at the same rate of energy, emphasizing potential differences in impact responses. The velocity of the falling weight was adjusted as an experimental indicator using two types of falling weights, both with similar collision energy levels but various ratios of speed and mass. Table (2) provides a detailed list of these experimental variables, alongside the load capacities obtained from four-point static bending tests used to calculate static flexural capacity.

Drop weight impact tests were performed under uniform assumptions. Each specimen had a rectangular cross-section with the following dimensions: a width of (400 mm), a height of (500 - 800 mm), and a clear span length of (3300 mm). According to previous research [16], three longitudinal reinforcing bars each with a diameter of 32 mm, were positioned at the top and bottom, respectively.

Twelve rectangular RC beams made of GFRP, with dimensions of 100 x 150 mm in cross-section and a total length of 2400 mm, were fabricated according to the study by [35,63]. Two series made up the

experimental program. The flexural behavior of GFRP RC beams under static loading (four-point bending) was investigated using the first group of six beams. Key parameters examined included load-deflection behavior, energy absorption capacity, fracture patterns, and failure modes. The behavior of beams under impact loading (I) was investigated using the second series of six beams. The primary objective was to examine the effects of dynamic response forces, including inertial and support pressures, dynamic tensile strain of GFRP, impact forces, and mid-span deflections. The test variables were the concrete's compressive strength and longitudinal reinforcement ratio (ρ_f). There were three distinct rebar diameters utilized: 6.35 mm (#2), 9.53 mm (#3), and 12.7 mm (#4), offering 1.0%, 2.0%, and 0.5% reinforcement rates, respectively. The GFRP RC beams were designed for double reinforcement, with two GFRP bars in compression and two in each of the six tension zones.

All seven large-size beam specimens were prepared for drop hammer testing. As specified in [36], each beam has a 2000 mm span and a 168 mm rectangular cross-section. At each corner of the beam specimens, 12 mm diameter deformed bars were positioned in addition to the 25 mm-thick concrete overlay that had been applied. Stirrups, 10 mm in diameter and spaced 200 mm apart, were incorporated to enhance shear resistance. The test matrix variables were displayed in Table (3).

Ten large-scale beams were subjected to drop-weight tests as part of the experimental program [3], and three beams underwent baseline static loading tests. Every specimen in a series had the same reinforcing and geometrical arrangements. The impact weight (kg) and impact velocity (m/s) were specified alongside the series name for the drop weight test specimens. The calculations presented by (15) were utilized to calculate the impact weight and velocity. Test parameters had been shown at Tables (4) and (5).

Table 2. [16] Details of test variables

Series	Designation	Drop weight momentum (t·m/s)	Impact energy (kJ)	Compressive strength (MPa)	Cross section height (mm)	Static flexural capacity (kN)
1	E30-C40-H6-M1	9.33	30	40	600	735
2	E30-C40-H5-M1	9.33	30	40	500	715
3	E30-C28-H6-M1	9.33	30	28	600	553
4	E30-C28-H8-M1	9.33	30	28	800	938
5	E50-C40-H6-M1	12.04	50	40	600	716

Table 3. [36] The test specimen matrix.

Type	Drop height (m)	Impact velocity (m/s)	Hammer mass (kg)	Clear span (m)
RC-a	0.5	3.13	641	1.4
B15-a	0.5	3.13	641	1.4
B20-a	0.5	3.13	641	1.4
T15B15-a	0.5	3.13	641	1.4
RC-b	0.25/0.25	2.21/2.21	641	1.4
B20-b	0.25/0.25	2.21/2.21	641	1.4

Table 4. [3] Primary test parameters.

Specimen	Compressive strength of concrete (MPa)	Impact weight (kg)	Impact velocity (m/s)
BS	23.80	-	-
B-1.700-4.60	27.01	1.700	4.60
B-1.300-5.56	30.61	1.300	5.56
B-1.052-6.4	27.90	1.052	6.40
B-868-7.14	24.76	868	7.14
CS	27	-	-
C-1.700-4.60	32.14	1.700	4.60
C-1.300-5.56	30.25	1.300	5.56
C-868-7.14	26.26	868	7.14
DS	24.80	-	-
D-1.700-4.60	32.73	1.700	4.60
D-1.300-5.56	25.59	1.300	5.56
D-868-7.14	25.01	868	7.14

Table 5. Surface condition between specimens and impactor of previous studies.

Reference	Impact force measure	Reaction force	Negative reaction force	Sampling rate (kHz)	Data processing	Contact condition	Impactor shape
Pham and Hao [44]	Load cell on beam	Two load cells	Yes	50	-	Steel plate	Hemispherical
Pham and Hao [45]	Load cell on beam	Two load cells	None	50	-	Steel plate	Hemispherical
Saatci and Vecchio [6]	Indirect	One load cell	None	2.4	-	Steel plate	flat
Kishi et al. [28,46]	Incorporated load cell	One load cell	None	-	-	-	Hemispherical
Kishi and Mikami [32]	Incorporated load cell	One load cell	-	40	Moving window	Direct	Hemispherical
Wang et al. [47]	Incorporated load cell	No restrain and no load cell	None	100	Cut off frequency of 6.2 kHz	Direct	Curved
Reference	Impact force measure	Reaction force	Negative reaction force	Sampling rate (kHz)	Data processing	Contact condition	Impactor shape
Tang and Saadatmanesh [48]	-	One load cell	None	-	-	-	Curved
Fujikake et al. [15]	Incorporated load cell	-	-	100	-	Direct	Hemispherical

Reference	Impact force measure	Reaction force	Negative reaction force	Sampling rate (kHz)	Data processing	Contact condition	Impactor shape
Bhatti et al. [49]	Incorporated load cell	One load cell	None	40	-	Direct	Hemispherical
Banthia et al. [50]	Incorporated load cell	One load cell	None	5	-	Direct	-
Hughes and Mahmood [51]	- .3+369584	One load cell	-	-	-	-	-
Zhao et al. [52]	Incorporated load cell	One load cell	Yes	100	-	Steel plate	Hemispherical
Zhan et al. [53]	Incorporated load cell	-	-	250	-	Rubber pad	Flat, wedge type
Wu et al. [54]	Load cell on beam	No restraint	-	100	Cut off 5 kHz	pad	Hemispherical
Tang and Saadatmanesh [55]	-	Restrained and load cell	None	-	-	Direct	Curved
Tachibana et al. [56]	Incorporated load cell	Restrained and load cell	-	20	-	Direct	Curved
Soleimani and Banthia [57]	Incorporated load cell	Restrained and load cell	None	100	-	Direct	Curved, wedge type
Silva et al. [58]	Incorporated load cell	No load cell	-	-	-	Direct	Spherical ball
Liu and Xiao [59]	Incorporated load cell	Restrained and load cell	None	100	Cut off 6 kHz	Direct	Flat
Hughes and Beeby [60]	Incorporated load cell	Restrained and load cell	-	-	-	Various pads	Spherical ball
Goldston et al. [61]	Incorporated load cell	Restrained and load cell	None	50	-	-	Direct
Bhatti and Kishi [62]	Incorporated load cell	Restrained and load cell	-	40	Moving window	Direct	Curved

2.2. TEST SETUP AND PROCEDURES

A steel impactor elevated to a certain height is dropped into a concrete beam or other element as part of drop-weight impact tests. A drop hammer machine [16] was used to test Series S1616 beam specimens with a 400 kg mass at four distinct heights: 0.15 m, 0.3 m, 0.6 m, and 1.2 m. Series SI322 beam specimens were tested at heights of 0.3 m, 0.6 m, 1.2 m, and 2.4 m. In order to determine the contact force created between the hammer and the RC beam, a dynamic load cell was employed. Additionally, a laser displacement sensor was utilized to capture the mid-span deflection response of the RC beam. To measure the reaction, a sensor affixed a thin rubber sheet to the underside of the RC beam. A computer-based data acquisition system recorded the data at a sampling rate of 100 kHz.

RC beams were subjected to drop weight impact tests at two energy levels, 30 and 50 kJ, by [16, 31].

Following the impact tests, static flexural testing was conducted to evaluate the residual performance of the beams damaged during impact. A concrete sapling had been revealed at the top surface and positioned at the loading points of the flexural test.

The weight was dropped onto the beam specimen in the drop weight impact test at a height determined to fulfill the desired impact energy. There were three distinct drop weights utilized for

0.7, 1.5, and 2.5 tons were tested. The steel weights had a 1010 mm radius of curvature and were shaped like spherical rocks, as investigated in [16]. The falling weight test analyzed the collision force, delay force, response force, and displacement to determine the collision response. Two accelerometers were installed in order to measure the impact and inertia forces. five beams spaced 400 mm apart from the center, and five weights' head. To determine the collision force, divide the acceleration by the mass of the dropped weight. The RC beam was mounted with five accelerometers,

as indicated in Fig. 2 of the drop weight test configuration. Every accelerometer determined the beam's acceleration in a certain area.

Six GFRP RC beams were exposed to collision stresses using the drop hammer technique [35], as depicted in Fig. 3. Two concrete blocks were anchored in place to allow the beams to be easily supported and subjected to three-point dynamic loads. To determine beam resistance, load cells were calibrated and placed beneath the concave rollers on both supports of the GFRP RC beams. Every support has rubber bands around it to keep the GFRP RC beams from bouncing when they were hit.

Fig. 4 depicts the arrangement of the drop hammer impact test and the equipment placement in the beam specimens. The drop hammer machine has a drop hammer frame [36], a clamping system, and a measuring system. The drop hammer structure weighs 641 kg. By attaching weight bricks to the frame, a higher weight may be set. The design called for a maximum drop height of 5 meters. A bolt-fixed load cell with a 1.2 MHz sampling rate was installed between the drop hammer frame and the indenter. The research used a 100 mm diameter hemispherical indenter. The release system will cause the drop hammer to descend freely along the guiding rails. The totally fixed boundary conditions were intended to be provided by the clamping system. LVDTs, high speed camera and IL Series multifunction laser sensor were used to measure the deflection of test beam specimens.

Fig. 5 displays the experimental setup as it was created by [3]. An impact hammer could be dropped by the mechanism up to three meters in the air. The hammer's whole construction was composed of steel. The dropping hammer's striking head has a 500 mm radius hemispherical tip. The number of steel plates may be varied to change the weight. To measure the

load, a 2 MN load cell was mounted on the drop hammer. The primary mechanism regulating the drop hammer's descent was an automated unhooking device mounted atop the drop weight. The identical simply supported testing conditions were applied to each specimen. A hollow steel beam was placed on top of the supports to prevent them from rising during the impact loading test.

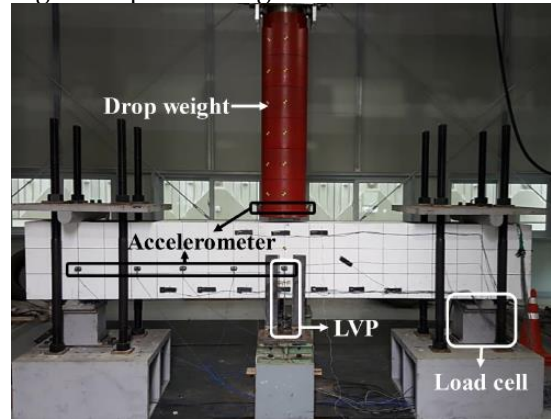


Fig. 2. Test setup for the falling weight collision test [16].

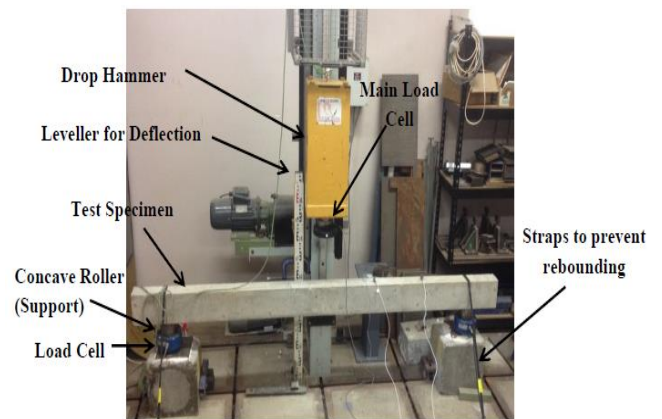


Fig. 3. Impact testing apparatus [35].

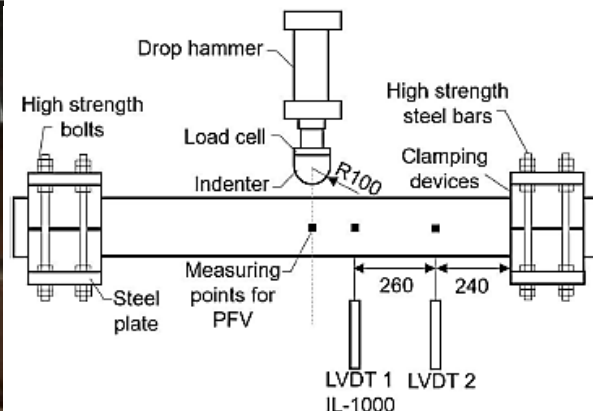
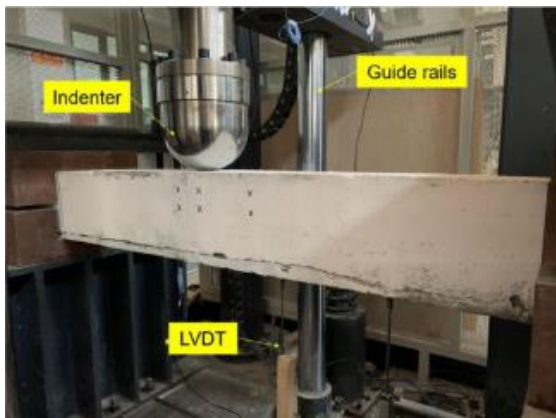


Fig. 4. The drop hammer impact instrumentation [36]

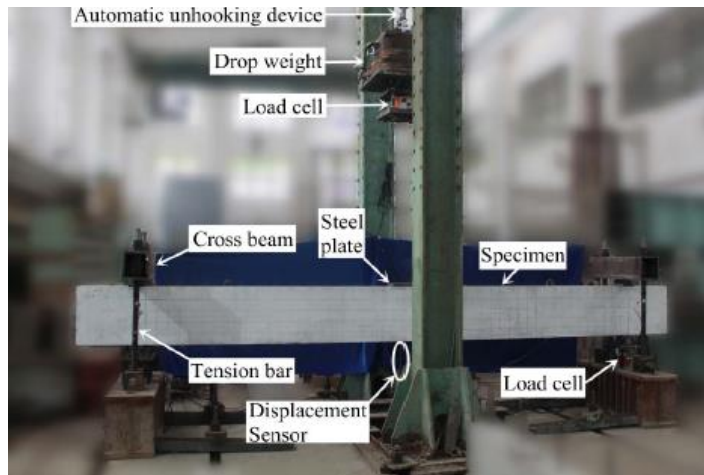


Fig. 5. Experimental setup [3]

3. TEST FINDINGS AND DISCUSSION

3.1. FAILURE MODES AND PATTERNS OF CRACKS

All specimens were intended to show ductile flexural failure mechanisms when subjected to static loading. Nevertheless, in all test situations, the beams' impact loading [3, 16, 30] induced crack patterns that differed from their typical static loading-induced crack patterns, and Fig. 6 illustrates an example case

following collision. The following three phenomena were seen in the crack patterns. (1) The main diagonal cracks that formed the shear plug originated from the upward and went downhill, with the majority of the cracks confined toward the mid-span or much below the beam's impact point. Subsequent to the shear plug's formation. (2) Multiple diagonal shear fractures parallel to the plug appeared among support and mid-span. (3) Cracks within particular samples beginning at the upper surface of the beam between the support and the impact location due to the inertia force's negative bending moment.

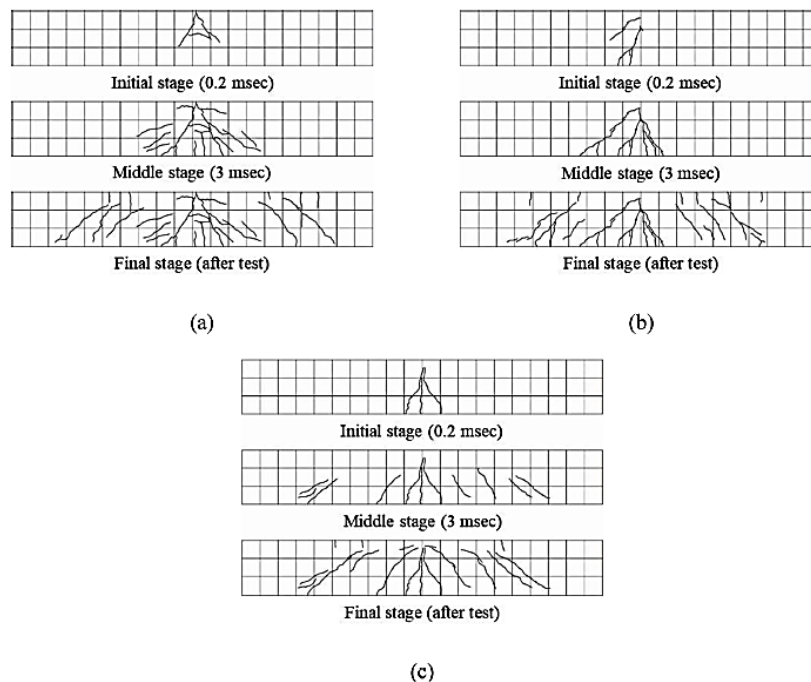


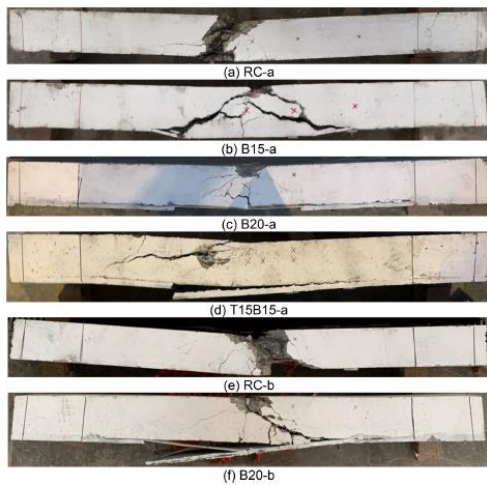
Fig. 6. Crack propagation of series 1 (a) Mass 1; (b) Mass 2; (c) Mass 3 [16].

Figs. 7a and 7b demonstrate how impact loading causes all beams to fail. Beam specimens' shear failure patterns revealed two distinct series. Based on the observation of fracture formation, as indicated, (1)

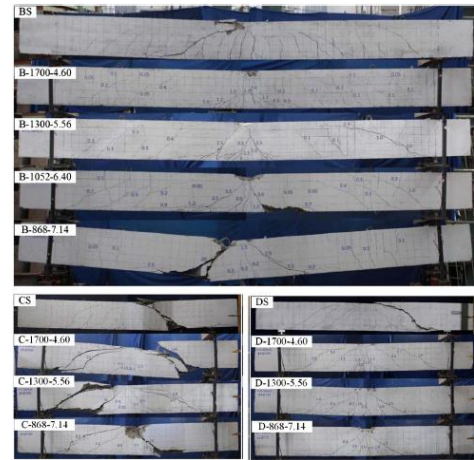
inclined fractures emerging in the shear span (Type II); (2) diagonal fractures growing into the shear plug (Type I). According to Zhao et al. [3], Type II fractures were the predominant failure cracks when the

beam specimens had been subjected to comparatively mild impact energy. Type I fractures were increasingly noticeable and eventually became dominant failure

cracks when the imported kinetic energy increased, whereas Type II cracks were insignificant or barely apparent.



(a) Failure patterns under impact loading [36].



(b) Failure patterns under impact loading [3]

Fig. 7. Failure patterns under impact loading of all tested beams [3].

3.2. MID-SPAN HISTORY REACTION DEFLECTION-TIME

Impact force rapidly dropped to zero after reaching a peak, as seen in Fig. 8a, giving rise to nearly triangular-shaped time history responses. Both the pre and post peak periods had negative impact force and variance, with the post-peak period exhibiting the greatest number of peaks of negative impact force. The drop weight's instant access with the beam, the length of the signal line, and the materials utilized, all of which create significantly high-frequency noise, influenced the accelerometer's sensitivity in the impact test [16]. Additionally, the same behavior was noted in earlier research, the impact force was measured using an accelerometer [6, 37, 38]. The beam's inertia force, caused by its acceleration, is what mostly opposes the impact force when the drop weight collides with the RC beam. As seen in Fig. 8b, because of the beam's oscillation, the

inertia force first approaches zero. The inertia force is then periodically reversed until it approaches zero. The reaction forces were relatively tiny as compared to the impact force's peak values, as observed in Fig. 8c. Furthermore, the reaction force's time history response after reaching its peak was the same as that of the inertia force because the impact force converged to zero quicker than the inertia force created. Because the steel plate placed on top of the beam tightened it, the load cell received both the bearing force and the self-weight of the RC beam. Previous research [12, 13, 38, 40] has observed and analyzed this phenomenon. As demonstrated in Fig. 8d, until the amplitude converged to a particular value, the deflection over time displayed a half-sine wave pattern.

Table 6 presents the findings of the drop hammer impact test [36]. enhancement.

Table 6. Impact test results [36].

Series	Peak impact force (KN)	Impulse (KN.s)	Peak mid-span displacement(mm)	Residual displacement(mm)	Peak disp. Lvdt1	Peak disp. Lvdt2
RC-a	212.4	3.17	-	-	48.77	32.54
B15-a	208.9	3.07	54.03	34.98	42.38	28.86
B20-a	211.3	3.11	47.16	29.35	37.33	25.07
T15B15-a	227.4	3.28	44.41	30.61	34.58	23.39
RC-b (1 st)	137.5	2.07	34.41	24.72	26.47	17.11
RC-b (2 nd)	108.1	2.15	35.19	17.92	28.69	18.62
B20-b (1 st)	160.75	2.11	21.93	8.77	15.99	10.11
B20-b (2 nd)	166.18	2.25	27.29	12.53	19.61	11.69

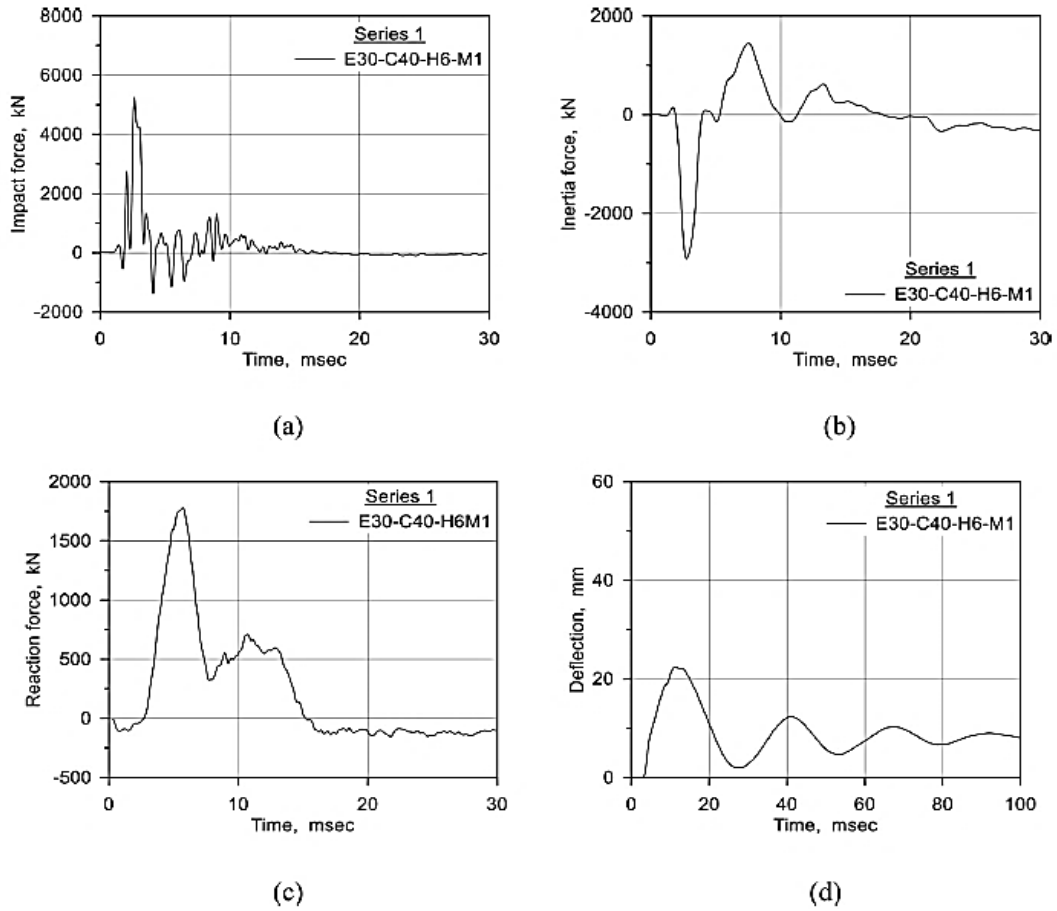


Fig. 8. Time historical responses: (a) Impact force; (b) Inertia force; (c) Reaction force; and (d) Deflection [16].

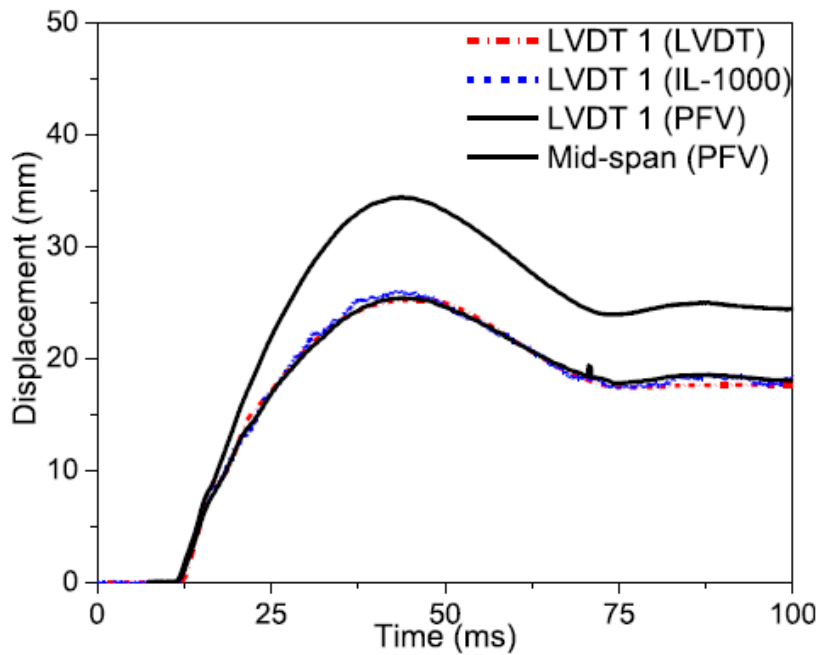


Fig. 2. A comparative analysis of RC-b's displacement time history (initial impact) [36].

4. EFFECT OF LOAD AND DISPLACEMENT ON THE NATURAL FREQUENCY OF A SPECIMEN

A function of the three variables was developed to study the impact of load and displacement on the natural frequency of a test part [42]. We were able to precisely determine the natural frequency of a test subject in real time thanks to this feature. A test member's rigidity varied over time during reciprocating movement due to deterioration. Stiffness, denoted by $k(t)$, is a function of time. The symbols $f(t)$ and $y(t)$ denote the displacement of the test member and the load applied to it, which are both functions of time. The definition of stiffness connects these three quantities.

$$f(t) = y(t) \cdot k(t) \quad (1)$$

Equation (1) has been applied through elastic to plastic stages. The force producing the same displacement enters a plastic condition and keeps falling as structural deterioration grows. The function $k(t)$ represents global stiffness. The structural natural frequency (circular frequency) has been calculated by Eq. 2.

$$w^2 = \frac{k}{m} \quad (2)$$

The quality of a test member m changed very little with stress and damage, therefore it was considered constant. The damaging process caused a modification in the natural frequency. As a result, it is a time-dependent function, indicated by $w(t)$. Consequently, Eq. 2 might be written as.

$$[w(t)]^2 = \frac{k(t)}{m} \quad (3)$$

After inserting Equation (1) into Equation (3), Equation (4) was discovered.

$$w(t) = \sqrt{\frac{k(t)}{m}} = \sqrt{\frac{f(t)}{y(t) \cdot m}} \quad (4)$$

4.1. IMPACT VELOCITY

The overall speed of an object when it falls from a specific height and impacts the ground or another object is known as the impact velocity. The hammer's velocity (V_h) at impact is computed using Equ. 5 [43].

$$V_h = \sqrt{2gh} \quad (5)$$

In this equation, V_h represents the velocity of the falling hammer at impact (m/s), g represents the acceleration due to gravity equals 9.81 m/s², and h represents the drop height (m).

4.2. FALLING FORCE

When an object's mass causes an inertial reaction and gravity's acceleration add up to a net downward acceleration, this is known as a falling force. In other words, a falling force is a net force acting on an object that is falling from a certain point. The Falling Force can be computed using the following formula Eq.6.

$$F_f = GF - AF \quad (6)$$

Where F_f is the net force exerted on a free-falling object (N), $GF = \text{mass} \cdot 9.81 \text{m/s}^2$, and $AF = \text{force of air resistance (N)}$.

4.3. THE FORMULA FOR FREE FALL DISTANCE

As indicated in Eq. 7, Free Fall Distance formula.

$$FFD = 0.5 \cdot g \cdot t^2 \quad (7)$$

Where FFD is the Free Fall Distance (m), t is the total time of free fall (sec), g is the acceleration due to gravity (9.81 m/s²).

4.4. THE FORMULA FOR FREE FALL DISTANCE

Kinetic energy (K_E) is exactly associated with an object's mass and the square of its velocity, as demonstrated in Eq. 8.

$$K_E = 1/2 m v^2 \quad (8)$$

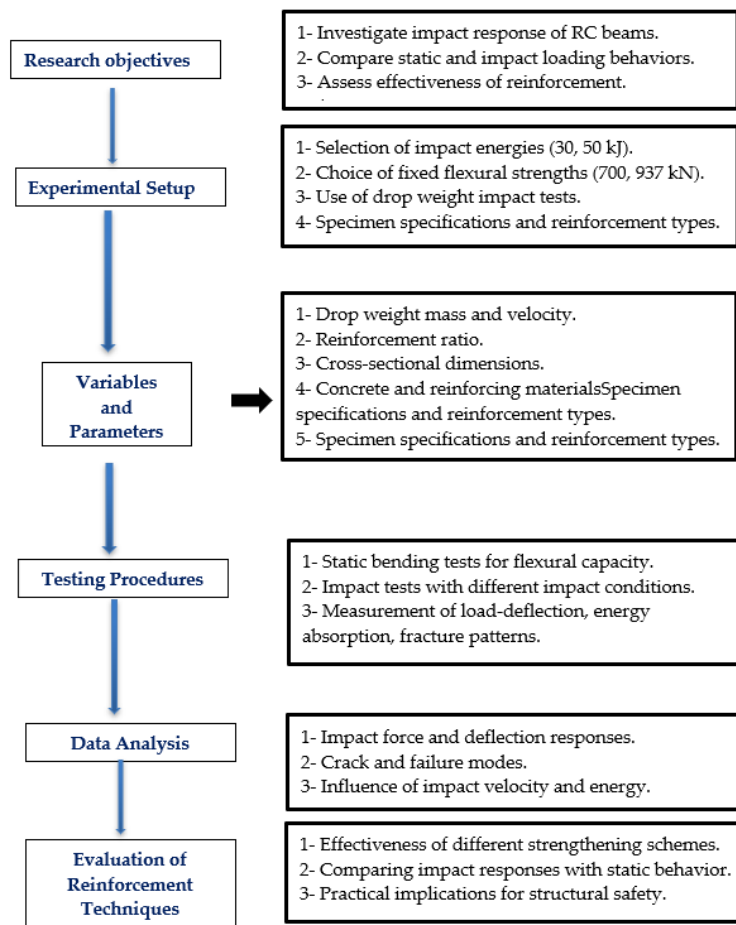
If the mass is in kilograms and the velocity is in meters per second, then the kinetic energy is measured in kilograms-meters squared per second. Joules (J) are widely used units of measurement for kinetic energy.

The force exerted on the two objects determines the potential energy formula. Eq. 9 shows the formula for the gravitational force.

$$P.E. = nmgh \quad (9)$$

where h is the height in meters, Gravity's acceleration is denoted as g (9.8 m / s²), and m is the mass in kilograms. It's important to note that the units for gravitational potential energy are $\text{kg} \cdot \text{m}^2 / \text{s}^2$, which correspond to kinetic energy. Actually, the Joule (J) unit of measurement is used to measure all energy, and it has the same units: $\text{kg} \cdot \text{m}^2 / \text{s}^2$

5. A FLOWCHART PRESENT THE RESEARCH PLAN AND OBJECTIVES



6. RECOMMENDATIONS FOR FUTURE RESEARCH

- Developing standardized impact testing methods and data reporting to enable better comparison across studies.
- Investigating the effects of repeated impacts and long-term durability of reinforcement strategies.
- Extending research to full-scale and real-world structures to validate laboratory findings.
- Exploring environmental influences and the performance of innovative, sustainable reinforcement materials.
- Integrating multi-hazard analysis to design more resilient structural elements.

Focusing on these gaps can help advance the understanding of impact behavior in RC beams and improve design practices for impact-resistant structures.

7. CONCLUSIONS

1. When subjected to impact loads, RC beams behaved differently from when subjected to static loading. Diagonal shear cracks in particular were crucial to the overall behavior.
2. Reinforced concrete beams' impact behavior is influenced by factors such as energy, cross-section size, flexural capability, drop weight progress, and strength.
3. In RC beams subjected to impact loading, noticeable diagonal shear cracks (Type I cracks) appeared close to the loading site. The primary distinction between studies that were quasi-static and dynamic was this defining aspect.
4. Strengthening materials and sustainable internal reinforcement can improve structural behavior and increase ultimate capacity under static loads.

REFERENCES

- [1] Thong M Pham and Hong Hao. Prediction of the impact force on reinforced concrete beams from a drop weight. *Advances in Structural Engineering* (1–13), (2016).
- [2] Huawei Li, Wensu Chen, Hong Hao. Influence of drop weight geometry and interlayer on impact behavior of RC beams, *International Journal of Impact Engineering* 131 222–237(2019).
- [3] Zhao D, Yi W, Kunnath SK. Shear mechanisms in reinforced concrete beams under impact loading. *J Struct Eng*;143(9):04017089(2017).
- [4] Yan Q, Sun B, Liu X, Wu J. The effect of assembling location on the performance of precast concrete beam under impact load. *Adv. Struct. Eng.*;21(8):1211–22 (2018).
- [5] Pham TM, Hao Y, Hao H. Sensitivity of impact behaviour of RC beams to contact stiffness. *Int J Impact Eng*;112:155–64 (2018).
- [6] Saatci, S. and Vecchio, F.J. Effects of shear mechanisms on impact behavior of reinforced concrete beams. *ACI Structural Journal*, 106(1), 78–86, (2009).
- [7] Chen Y, May IM. Reinforced concrete members under drop-weight impacts. *Proc. Inst Civil Eng Struct Build*;162(1):45–56,(2009).
- [8] Adhikary SD, Li B, Fujikake K. Low velocity impact response of reinforced concrete beams: experimental and numerical investigation. *Int J Protective Struct*;6(1):81–111,(2015).
- [9] Anil Ö, Durucan C, Erdem RT, Yorgancilar MA. Experimental and numerical investigation of reinforced concrete beams with variable material properties under impact loading. *Construct Build Mater*;125:94–104,(2016).
- [10] Yilmaz M, Anil Ö, Alyavuz B, Kantar E. Load displacement behavior of concrete beam under monotonic static and low velocity impact load. *Int J Civil Eng*;12(4):488–503,(2014).
- [11] Zhan T, Wang Z, Ning J. Failure behaviors of reinforced concrete beams subjected to high impact loading. *Eng Fail Anal*;56:233–43, (2015).
- [12] Tachibana S, Masuya H, Nakamura S. Performance based design of reinforced concrete beams under impact. *Nat Hazards Earth Syst Sci*;10(6):1069–78,(2010).
- [13] Kishi N, Mikami H. Empirical formulas for designing reinforced concrete beams under impact loading. *ACI Struct J*;109(4):509–19,(2012).
- [14] Kishi N, Mikami H, Matsuoka KG, Ando T. Impact behavior of shear-failure-type RC beams without shear rebar. *Int J Impact Eng*;27(9):955–68,(2002).
- [15] Fujikake K, Li B, Soeun S. Impact response of reinforced concrete beam and its analytical evaluation. *J Struct Eng*;135(8):938–50,(2009).
- [16] Yu, Y., S. Lee, and J.-Y. Cho. “Deflection of reinforced concrete beam under low-velocity impact loads.” *Int. J. Impact Eng.* 154 (Aug):103878,(2021).
- [17] Xu S, Liu Z, Li J, Yang Y, Wu C. Dynamic behaviors of reinforced NSC and UHPC columns protected by aluminum foam layer against low-velocity impact. *J Build Eng*;34:101910,(2021).
- [18] Fan W, Shen D, Yang T, Shao X. Experimental and numerical study on low-velocity lateral impact behaviors of RC, UHPFRC and UHPFRC-strengthened columns. *Eng Struct*;191:509–25,(2019).
- [19] Brühwiler E, Denari’e E. Rehabilitation and strengthening of concrete structures using ultra-high performance fibre reinforced concrete. *Struct Eng Int*;23:450–7,(2013).
- [20] Habel K, Denari’e E, Brühwiler E. Experimental investigation of composite ultrahigh-performance fiber-reinforced concrete and conventional concrete members. *ACI Struct J*;104:93,(2007).
- [21] Safdar M, Matsumoto T, Kakuma K. Flexural behavior of reinforced concrete beams repaired with ultra-high performance fiber reinforced concrete (UHPFRC). *Comp.Struct*;157:448–60,(2016).
- [22] Al-Osta M, Isa M, Baluch M, Rahman M. Flexural behavior of reinforced concrete beams strengthened with ultra-high performance fiber reinforced concrete. *Constr Build Mater*;134:279–96, (2017).
- [23] Yongjae Yu, Sangho Lee, Hyukjun Ahn and Jae-Yeol Cho. Residual Performance of Reinforced Concrete Beams Damaged by Low-Velocity Impact Loading. *J. Struct. Eng.*,149(3),(2023).
- [24] Adhikary, S. D., B. Li, and K. Fujikake. 2012. “Dynamic behavior of reinforced concrete beams under varying rates of concentrated loading.” *Int. J. Impact Eng.* 47, 24–38, 02.001,(2012).
- [25] Adhikary, S. D., B. Li, and K. Fujikake. “Effects of high loading rate on reinforced concrete beams.” *ACI Struct. J.* 111 (3): 651–660,(2014).
- [26] Adhikary, S. D., B. Li, and K. Fujikake. “Low velocity impact response of reinforced concrete beams: Experimental and numerical investigation.” *Int. J. Prot. Struct.* 6 (1): 81–111,(2015a).
- [27] Adhikary, S. D., B. Li, and K. Fujikake. “Residual resistance of impact-damaged reinforced concrete beams.” *Mag. Concr. Res.* 67 (7):364–378,(2015b).

- [28] Kishi, N., O. Nakano, K. G. Matsuoka, and T. Ando. "Experimental study on ultimate strength of flexural-failure-type RC beams under impact loading." In Proc., 16th Int. Conf. on Structural Mechanics in Reactor Technology, 1-7. Washington, DC: International Association for Structural Mechanics in Reactor Technology,(2001).
- [29] Hwang, H. J., F. Yang, L. Zang, J. W. Baek, and G. Ma. "Effect of impact load on splice length of reinforcing bars." *Int. J. Concr. Struct. Mater.* 14 (1): 1-17,(2020).
- [30] Yu YJ. Response of RC beam subjected to low velocity impact loading, phd thesis. Seoul, South Korea: Department of Civil & Environmental Engineering, Seoul National University; (2019).
- [31] Ahn, H. "Effect of flexural stiffness on impact behavior of RC beam subjected to low-velocity impact loading." Masters' thesis, Dept. of Civil and Environmental Engineering, Seoul National Univ,(2021).
- [32] Kishi N, Mikami H. Empirical formulas for designing reinforced concrete beams under impact loading. *ACI Struct J-Am Concr Inst*;109(4):509-19(2012).
- [33] Tachibana S, Masuya H, Nakamura S. Performance based design of reinforced concrete beams under impact. *Nat. Hazards Earth Syst Sci*;10(6):1069-78,(2010).
- [34] Zhan T, Wang Z, Ning J. Failure behaviors of reinforced concrete beams subjected to high impact loading. *Eng Fail Anal*;56:233-43,(2015).
- [35] Goldston, M., Remennikov, A. & Sheikh, M. Neaz. Experimental investigation of the behaviour of concrete beams reinforced with GFRP bars under static and impact loading. *Engineering Structures*, 113, 220-232, (2016).
- [36] Jie Wei, Jun Li, Chengqing Wu, Zhong-xian Liu and Jianguang Fang. Impact resistance of ultra-high performance concrete strengthened reinforced concrete beams. *International Journal of Impact Engineering*, 158, 104023, (2021).
- [37] Kishi N, Bhatti AQ. An equivalent fracture energy concept for nonlinear dynamic response analysis of prototype RC girders subjected to falling-weight impact loading. *Int J Impact Eng*;37(1):103-13, (2010).
- [38] Yoo DY, Banthia N, Kim SW, Yoon YS. Response of ultra-high performance fiber reinforced concrete beams with continuous steel reinforcement subjected to low velocity impact loading. *Composite Structures*;(126):233-45, (2015).
- [39] Cotsovos DM. A simplified approach for assessing the load-carrying capacity of reinforced concrete beams under concentrated load applied at high rates. *Int. J. Impact Eng*;*37*:907-917, (2010).
- [40] Bhatti AQ, Kishi N, Mikami H. An applicability of dynamic response analysis of shear-failure type RC beams with lightweight aggregate concrete under falling weight impact loading. *Mater. Struct.*, 44(1):221-31, (2011).
- [41] Kazunori Fujikake. Impact Performance of Ultra-High Performance Fiber Reinforced Concrete Beam and Its Analytical Evaluation. *International Journal of Protective structures*;(2014).
- [42] Zhenhao Zhang ,Feng Cao , Jianyu Yang , and Zhigang He. Experiment on Natural Frequency Change of Reinforced Concrete Members under Low Cycle Loading. *Shock and vibration*;(2018).
- [43] S.M. Soleimani, Banthia, N and Mindess, S. Behavior of RC beams under impact loading: some new findings. *FRACTURE MECHANICS OF CONCRETE AND CONCRETE STRUCTURES*.
- [44] Pham, T.M. and Hao, H. Impact behavior of prestressed RC beams under drop weight impact loads. *Materials and Structures*, 50, Article 23. (2017b).
- [45] Pham, T.M. and Hao, H. Failure of RC beams under lateral impact loads. *International Journal of Protective Structures*, 7(2), 183-210, (2016).
- [46] Kishi, N., Mikami, H., and Ando, T. Impact behavior of shear-failure-type reinforced concrete beams. *Proceedings of the JSCE*, 721, 115-129, (2002).
- [47] Wang, W.C., Weng, M.C., and Chao, S.H. Dynamic response of RC beams under low-velocity impact loading. *ACI journal*, (1996).
- [48] Tang, C. and Saadatmanesh, H. Behavior of reinforced concrete beams strengthened with FRP composites under impact loads. *ACI Structural Journal*, 102(5), 713-721, (2005).
- [49] Bhatti, A.Q., Kishi, N., and Mikami, H. Impact response of RC beams retrofitted with steel plates. *Journal of Advanced Concrete Technology*, 7(1), 71-85, (2009).
- [50] Banthia, N., Mindess, S., and Bentur, A. Impact resistance of concrete beams. *Materials and Structures*, (20), 293-298, (1987).
- [51] Hughes, T.G. and Mahmood, A. Impact resistance of reinforced concrete beams. *Proceedings of*

- the Institution of Civil Engineers, 77(2), 145–156, (1984).
- [52] Zhao, X., Lu, Y., Hao, H., and Ma, G. Experimental study of RC beams under impact loading. *International Journal of Impact Engineering*, 108, 26–39, (2017).
- [53] Zhan, Y., Li, J., and Ma, G. Experimental investigation on dynamic responses of concrete beams under impact. *Engineering Structures*, 84, 29–39, (2015).
- [54] Wu, C., Oehlers, D.J., Rebstrost, M., Grzebieta, R.H., and Whittaker, A.S. A review of impact loading tests on reinforced concrete beams. *International Journal of Structural Stability and Dynamics*, 15(2), (2015).
- [55] Tang, C. and Saadat manesh, H. Impact resistance of CFRP-retrofitted RC beams. *Composite Structures*, 61(1-2), 159–168, (2003).
- [56] Tachibana, E., Matsuzaki, Y., and Kishi, N. Dynamic response of RC beams under impact loads. *Journal of Advanced Concrete Technology*, 8(2), 205–215, (2010).
- [57] Soleimani, S.M. and Banthia, N. Performance of GFRP-sheathed RC beams under impact loading. *Journal of Composites for Construction*, 18(6), (2014).
- [58] Silva, P., Lu, Y., and Hao, H. Numerical simulation of reinforced concrete slab under impact loading. *International Journal of Impact Engineering*, 36(10-11), 1213–1224, (2009).
- [59] Liu, J. and Xiao, Y. Impact behavior of concrete beams strengthened with carbon fiber sheets. *Construction and Building Materials*, 152, 138–151, (2017).
- [60] Hughes, T.G. and Beeby, A.W. Impact behavior of reinforced concrete beams. *Magazine of Concrete Research*, 34(121), 141–152, (1982).
- [61] Goldston, M., Remennikov, A.M., and Sheikh, M.N. Experimental investigation of RC beams under impact loads. *International Journal of Impact Engineering*, 95, 27–40, (2016).
- [62] Bhatti, A.Q. and Kishi, N. Experimental and numerical investigation of RC beams retrofitted with steel plates. *Journal of Advanced Concrete Technology*, 9(3), 229–243, (2011).
- [63] Sabry Fayed. Effect of Aluminum Alloy Sheets on structural behavior of RC Beams. *Journal of Contemporary Technology and Applied Engineering*, 1(1), Pages 39-48,(2022).